Evolutionary loss of foot muscle during development with characteristics of atrophy and no evidence of cell death

Mai P. Tran[1], Rio Tsutsumi[1], Joel M. Erberich[1], Kevin D. Chen[1], Michelle D. Flores[1], and Kimberly L. Cooper[1,2,*]

[1]Division of Biological Sciences, Section of Cellular and Developmental Biology, University of California San Diego, La Jolla, California 92093, USA.

[2]Lead Contact

[*]Correspondence: kcooper@ucsd.edu

Summary

Many species that run or leap across sparsely vegetated habitats, including hooved animals like horses and deer, evolved the severe reduction or complete loss of foot muscles as skeletal elements elongated and digits were lost. Although entire groups of muscles were lost repeatedly throughout vertebrate evolution, the developmental mechanisms remain unknown. Here, we report the natural loss of intrinsic foot muscles in a small bipedal rodent, the lesser Egyptian jerboa (*Jaculus jaculus*). Although adults have no muscles in their feet, the early stages of myoblast migration and fusion proceed normally to form multinucleated myofibers in most anatomical locations that are orthologous to other rodents. However, all cells with muscle identity rapidly disappear soon after birth. We were surprised to find no evidence of apoptotic or necrotic cell death and no stimulation of a local immune response during stages of peak myofiber loss. We instead see hallmarks of muscle atrophy, including an ordered disassembly of the sarcomere apparatus associated with upregulation of the E3 ubiquitin ligases, *MuRF1* and *Atrogin-1*. We propose that the natural loss of muscle, which remodeled foot anatomy during evolution and development, involves cellular mechanisms that are typically associated with disease or injury.

Results

Muscles in the feet of birds, reptiles, and mammals were lost multiple times in the course of limb evolution, usually coinciding with the loss of associated digits and elongation of remaining skeletal elements [1–3]. However, the developmental mechanisms that lead to the natural absence of adult limb muscle are not known. We focused on the bipedal three-toed jerboa, a small laboratory rodent model for evolutionary developmental biology, to determine if evolutionary muscle loss conforms to expectations based on what was previously known about

muscle cell biology. The hindlimb architecture of the adult jerboa is strikingly similar to the larger and more familiar hooved animals, including the disproportionately elongated foot that lacks all intrinsic muscle [2,3]. The tendons were retained and expanded in each of the anatomical positions where flexor muscles are absent (Figures 1A, 1B and S1A-F) and serve to resist hyperextension when the terminal phalanx contacts the ground during locomotion [4,5].

The absence of intrinsic foot muscle in the adult jerboa could be due to a failure of early myoblasts to migrate into and/or to differentiate in the distal limb. Alternatively, embryonic muscles may form but not persist through development to the adult. In transverse sections of newborn mouse feet, immunofluorescent detection of skeletal muscle myosin heavy chain reveals each intrinsic muscle group (Figure S1G). In newborn jerboas, we observed two of the three groups of flexor muscles. While the *m. lumbricales* never form, the jerboa has a single *m. flexor digitorum brevis* and three pinnate *m. interossei* that are not present in adults (Figure S1H).

Postnatal growth of vertebrate skeletal muscle typically involves an increase in myofiber number (hyperplasia) within the first week, followed by an increase in myofiber size (hypertrophy) [6–8]. In order to understand the dynamics of muscle growth and loss, we quantified the rate of myofiber hyperplasia at two-day intervals after birth of the mouse and jerboa, focusing on the representative interosseous muscle that is associated with the third metatarsal (Figures 1E, F). As expected in the mouse, we observed a steady increase in the average number of myofibers in cross section from birth to P8 (Figure 1C). In contrast, the number of myofibers in the third interosseous of the jerboa foot initiate a rapid decline at around P4, and few myofibers remain by P8 (Figure 1D).

It is possible that the rate of myofiber loss outpaces a typical rate of new cell addition such that muscles with the potential to grow are instead steadily diminished. Alternatively, myofiber loss may be accelerated by a compromised ability to form new myofibers and to add nuclei to growing myofibers. To distinguish these hypotheses, we analyzed cohorts of animals two days after intraperitoneal BrdU injection at P0, P2, or P4. Since multinucleated jerboa foot myofibers are postmitotic (Figures S1I, J), we reasoned that BrdU+ nuclei present within Dystroglycan+ myofiber membranes were added by myocyte fusion during the two-day window after they were labeled as myoblasts or myocytes in S-phase (Fig. 2A). When normalized to the total number of myofiber nuclei, we found that myocytes fuse to form multinucleated myofibers in jerboa hand muscle at a consistent rate from P0 to P6. However, their incorporation into jerboa foot muscle decreased significantly after P2 (Fig. 2B). These results suggest that myofiber loss, which is initiated at P4, is preceded by reduced myogenesis.

The rapid and almost complete loss of differentiated myofibers from P4 to P8 suggested these cells die, since individual cells or groups of cells are commonly eliminated by apoptosis during development [9,10]. We therefore tested the hypothesis that neonatal intrinsic foot muscles undergo apoptosis by implementing the TUNEL assay to detect DNA fragmentation and by immunofluorescent detection of cleaved Caspase-3, a key protein in the apoptotic program [11]. Each revealed keratinocyte apoptosis in hair follicles that are known to undergo programmed cell death as a positive control in the same tissue sections [12]. However, TUNEL or cleaved Caspase-3 positive jerboa foot myofibers or cells in their vicinity were an extreme rarity (0.25% of myofibers) in animals ranging from P0 to P8 suggesting these cells do not die by apoptosis (Figures 3A, B, and S2).

Alternatively, myofiber loss may occur through a cell death mechanism that is first characterized by plasma membrane permeability, such as necrosis [13]. To test this hypothesis, we injected Evans blue dye (EBD), a fluorescent molecule that accumulates in cells with compromised plasma membranes [14,15], into the peritoneum of P3 and P4 neonatal jerboas 24 hours before euthanasia. Although we detected EBD in mechanically injured myofibers of the gastrocnemius as a control, we saw no EBD fluorescence in jerboa foot myofibers or in surrounding cells (Figures 3C and S3). We also saw no Annexin V immunofluorescence on the surface of jerboa foot myofibers, another hallmark of dying cells that flip Annexin V to the outer plasma membrane (Figures 3D and S3).

Since we observed no direct evidence of cell death, we asked whether there was an immune response that might be an indirect proxy for undetected death. Dying muscle cells frequently recruit phagocytic macrophages that engulf cellular debris [16–18]. We predicted that myofibers that die by any mechanism that produces cellular debris might recruit tissue resident macrophages that are detectable by expression of the F4/80 glycoprotein. However, consistent with the lack of evidence of cell death in the jerboa foot, no F4/80^{+} macrophages were found among myofibers from birth to P7 (Figures 3E and S4).

The absence of any clear indication of muscle cell death motivated us to re-evaluate muscle maturation at greater resolution in order to capture the earliest detectable signs of muscle cell loss. We collected transmission electron micrographs of jerboa hand and foot muscle at P0, P2, and P4. We identified criteria for three categories of maturation, as described previously [19–21], and two categories of degeneration. Category A cells have pre-myofibrils with thick and thin filaments and poorly resolved Z-discs, but the M-lines and I-bands are not yet apparent (Figure 4A). In Category B, Z-discs of nascent myofibrils are better resolved, and M-lines and I-bands are apparent, but parallel sarcomeres are not in register (Figure 4B). The

mature myofibrils of Category C have Z-lines that are aligned with one another (Figure 4C). In Category D, early degeneration, some sarcomeres appear similar to Category A, but other areas of the cell contain disorganized filaments (Figure 4D). Category E includes those in the worst condition where less than half of the cell has any recognizable sarcomeres, and much of the cytoplasm is filled with pools of disorganized filaments and Z-protein aggregates (Figure 4E). Additionally, Category D and E cells have membrane-enclosed vacuoles and large lipid droplets. However, consistent with a lack of evidence for cell death, none of these cells or their organelles appear swollen, nuclear morphology appears normal, plasma membranes seem to be contiguous, and we do not observe a large number of autophagic vesicles.

We then coded and pooled all images of hand and foot myofibers from P0, P2, and P4 jerboas and blindly assigned each cell to one of the five categories. Quantification of the percent of myofibers in each category after unblinding revealed the progressive maturation of jerboa hand myofibers and the progressive degeneration of jerboa foot myofibers (Figure 4G). Compared to later stages, there is little difference in the maturation state of hand and foot sarcomeres at birth. Loss of ultrastructural integrity is therefore initiated perinatally, prior to complete myofibril maturation in the jerboa foot.

Our analysis of transmission electron micrographs also revealed the presence of filamentous aggregates that we did not include in our quantifications because they are enucleate, lack all other recognizable organelles, and are not bounded by a plasma membrane. Although these aggregates do not appear to be cellular, they are always closely associated with cells of a fibroblast morphology, and most lie between remaining myofibers in a space we presume was also once occupied by a myofiber (Figures 4F, H). To determine if these unusual structures contain muscle protein, we performed immunofluorescence on sections of P4 jerboa foot muscle and found similar aggregates of intensely fluorescent immunoreactivity to skeletal muscle myosin heavy chain. We also found that the surrounding cells, which correlate with the positions of fibroblasts in electron micrographs, express the intracellular pro-peptide of Collagen I (Figure 4I), the major component of tendon and other fibrous connective tissues and of fibrotic tissue after injury [22].

Given the apparent deterioration of nascent sarcomeres, we asked whether individual sarcomere proteins are lost from myofibrils in a temporal order or if proteins disassemble simultaneously. We assessed the organization of sarcomere proteins by multicolor immunofluorescence at P0, P2, and P4. Alpha-Actinin, Desmin, Myomesin, Myosin, Titin, and Tropomyosin are each localized to an ordered series of striations in a subset of myofibers

suggesting all are initially incorporated into immature sarcomeres (Figure 5A and Table S1-5). By assessing all combinations of immunologically compatible primary antibodies, we identified populations of cells where Desmin was no longer present in an ordered array, but each of the other proteins appeared properly localized to the sarcomere (Figures 5B and Table S2). Although we could not distinguish such clear categories of mislocalization for each protein relative to all others, we inferred a relative timeline whereby Desmin disorganization is followed together by Myosin and Tropomyosin, then Titin, and lastly Myomesin and α-Actinin (Figures 5B-F and Tables S1-5).

Desmin forms a filamentous network that connects parallel sarcomeres to one another and coordinates myofibril contraction within cells and between neighboring cells [23–25]. In mouse models of muscle atrophy triggered by fasting or denervation, phosphorylation of Desmin removes the protein from the sarcomere and targets it for ubiquitination and proteolytic degradation prior to degradation of other sarcomere proteins [26]. The observation that Desmin is the first of an ordered sarcomere disassembly in the jerboa foot may reflect targeted degradation of muscle proteins that is similar to muscle atrophy.

The ubiquitin-proteasome system is the main pathway through which cellular proteins are degraded during muscle atrophy, and *MuRF1* and *Atrogin-1* are E3 ubiquitin ligases among the 'atrogenes' that are highly upregulated [27,28]. To test the hypothesis that muscle loss in the jerboa foot exhibits molecular hallmarks of atrophy, we performed quantitative reverse transcriptase PCR (qRT-PCR) of *MuRF1* and *Atrogin-1* mRNA from intrinsic foot muscles and the *flexor digitorum superficialis* (FDS) of the mouse and jerboa. The FDS, which originates in the autopod during embryogenesis and translocates to the forearm [29], is the most easily dissected of the analogous forelimb muscles and serves as a control for typical muscle maturation in both species.

When normalized to expression in the FDS at birth of each species, *Atrogin-1* expression is 3.1-fold higher in the jerboa foot at P3 (Figure 5G). *MuRF1* mRNA expression is already significantly elevated at birth and remains elevated at P3 (Figure 5H). The progressively disordered ultrastructure of the sarcomere that begins with loss of Desmin localization, the increased expression of *Atrogin-1* and *MuRF1*, and the lack of evidence for cell death or macrophage infltration are consistent with observations of atrophying muscle in mice and rats [26,30–32].

Despite these similarities to muscle atrophy, myofiber loss in the jerboa foot does not seem to be simply explained by an atrophic response to denervation. First, and in contrast to

the rapid rate of jerboa foot myofiber loss, chronic denervation in mice (100 days after nerve transection at P14) reduced the size but not the number of individual myofibers [33]. Additionally, we found that the post-synaptic Acetylcholine Receptor (AchR) exclusively coincides with the presynaptic neuronal protein, Synaptophysin, in neonatal jerboa foot muscles (Figure S5). In the mouse, AchR clusters are present in a broad domain of fetal muscle prior to innervation and are refined to nerve terminals in response to chemical synapse activity before birth [34]. The refinement of AchR clusters in jerboa foot muscles suggests that the muscles are not only innervated at birth but are also responsive to motor terminals.

Discussion

The natural process of muscle loss in the jerboa foot is surprising in the context of what is known about muscle development and pathology. Although we found multinucleated myofibers in the feet of neonatal jerboas, all muscle protein expression rapidly disappears from the jerboa foot shortly after birth. We were perplexed to find no evidence of apoptotic or necrotic cell death by a variety of assays and throughout the time when muscle cells are lost, nor did we observe macrophages that are commonly recruited to clear the remains of dying cells. Instead, we saw structural and molecular similarities to muscle atrophy, though atrophy in young mice leads to reduced myofiber size rather than number as in the jerboa [33,35].

Why would an embryo expend energy to form muscles that are almost immediately lost? The formation and subsequent loss of intrinsic foot muscles in jerboas, which also occurs in hooved animals [3], may simply reflect a series of chance events in each lineage with no fitness cost, or these similarities in multiple species may reveal true developmental constraints. Muscle is not required for autopod tendon formation or maintenance in mice, but the tendons that develop in a muscle-less or a paralyzed mouse are thinner and less well organized [36]. It is therefore possible that muscle is initially required in the fetus and neonate for tendons to establish sufficient architecture from origin to insertion so that the tendon, after further growth, can withstand high locomotor forces in the adult [4,5].

Regardless of whether these nascent muscles serve an essential purpose, we are left wondering what is the ultimate fate of jerboa foot myofibers. If these cells do indeed die, perhaps death is too rapid for detection. However, programmed cell death is thought to occur over hours or even days from the initial trigger to the final corpse [37]. Alternatively, death may result from a mechanism that does not proceed through DNA fragmentation, plasma membrane permeability, macrophage recruitment, or stereotyped ultrastructural changes, and yet this would seem to eliminate most known forms of regulated cell death [38]

Alternatively, multinucleated myofibers may transform to another cellular identity after degrading all sarcomere proteins. Although a fate transformation would be surprising, it would not be without precedent. The electric organ of fish that can produce an electric field (e.g. knifefish and elephantfish) is thought to be derived from skeletal muscle. Electrocytes of *Sternopygus macrurus* express skeletal muscle Actin, Desmin, and α-Actinin, and electrocytes of *Paramormyrops kingsleyae* retain sarcomeres that are disarrayed and non-contractile [39,40]. If myofibers in the jerboa foot indeed transdifferentiate, it is possible they transform into the pro-Collagen I positive fibroblasts that are entangled with the filamentous aggregates, though these could also be phagocytic fibroblasts recruited to consume the enucleate detritus without stimulating inflammation [41–44]. Unfortunately, the lineage labeling approaches required to track the ultimate fate of jerboa cells are exceptionally challenging in this non-traditional animal model.

It is clear, however, that regardless of the ultimate fate of jerboa foot myofibers, their path passes through a phase marked by cell biology that is typical of atrophy, including the ordered disorganization of sarcomeres and expression of the E3 ubiquitin ligases, *MuRF1* and *Atrogin-1*. However, skeletal muscle atrophy is typically associated with pathology in the context of disuse, nerve injury, starvation, or disease. In this context, we were struck by a statement in the 1883 anatomical description of the fetal and adult suspensory ligament of four species of hooved mammals: “It is an instance of *pathological* change assisting a *morphological* process” (emphasis his) [3]. Indeed, there are remarkable similarities in the histology of jerboa and horse foot muscle compared to human clinical observations of tissue remodeling that follows rotator cuff tear characterized by muscle atrophy, myofiber loss, and fibrosis [45,46].

Foot muscle atrophy in the jerboa may be one of many cellular responses associated with injury or disease in humans that is utilized in the normal development and physiology of other species. These data suggest that there is less of a clear divide between natural and pathological states than typically thought. Studies of non-traditional species may not only reveal the mechanisms of evolutionary malleability, but may also advance our understanding of fundamental biological processes that are typically associated with pathological conditions.

Acknowledgements

We thank V. Fowler, S. Lange, A. Sacco, S. Ward, D. Gokhin and R. Nowak for advice and for sharing reagents. M. Ellisman, Director of the National Center for Microscopy and Imaging Research at UC San Diego, and T. Deerinck, M. Mackey, and A. Thor provided assistance with transmission electron microscopy. H. Grunwald assisted with TUNEL staining. A. Mendelsohn

provided advice on the assessment of muscle innervation, and Y. Cho advised us on mouse muscle denervation. This work was funded by a Searle Scholar Award from the Kinship Foundation, a Pew Biomedical Scholar Award from the Pew Charitable Trusts, a Packard Fellowship in Science and Engineering from the David and Lucile Packard Foundation. M.P.T. was supported by the NIH Cell and Molecular Genetics training grant T32GM724039.

References

1. Abdala, V., Grizante, M.B., Diogo, R., Molnar, J., and Kohlsdorf, T. (2015). Musculoskeletal anatomical changes that accompany limb reduction in lizards. Journal of Morphology *276*, 1290–1310.

2. Berman, S.L. (1985). Convergent evolution in the hindlimb of bipedal rodents. Journal of Zoological Systematics and Evolutionary Research *23*, 59–77.

3. Cunningham, D.J. (1883). The Development of the Suspensory Ligament of the Fetlock in the Foetal Horse, Ox, Roe-Deer, and Sambre-Deer. Journal of anatomy and physiology *18*, i1–12.

4. Lochner, F.K., Milne, D.W., Mills, E.J., and Groom, J.J. (1980). In vivo and in vitro measurement of tendon strain in the horse. Am. J. Vet. Res. *41*, 1929–1937.

5. Moore, T.Y., Rivera, A.M., and Biewener, A.A. (2017). Vertical leaping mechanics of the Lesser Egyptian Jerboa reveal specialization for maneuverability rather than elastic energy storage. Frontiers in Zoology *14*, 32.

6. Chiakulas, J.J., and Pauly, J.E. (1965). A study of postnatal growth of skeletal muscle in the rat. The Anatomical record *152*, 55–61.

7. Gokhin, D.S., Ward, S.R., Bremner, S.N., and Lieber, R.L. (2008). Quantitative analysis of neonatal skeletal muscle functional improvement in the mouse. J. Exp. Biol. *211*, 837–843.

8. White, R.B., Biérinx, A.-S., Gnocchi, V.F., and Zammit, P.S. (2010). Dynamics of muscle fibre growth during postnatal mouse development. BMC developmental biology *10*, 21.

9. Fernández-Terán, M. a, Hinchliffe, J.R., and Ros, M. a (2006). Birth and death of cells in limb development: a mapping study. Developmental dynamics : an official publication of the American Association of Anatomists *235*, 2521–37.

10. Brill, A., Torchinsky, A., Carp, H., and Toder, V. (1999). The Role of Apoptosis in Normal and Abnormal Embryonic Development. J Assist Reprod Genet *16*, 512–519.

11. Elmore, S. (2007). Apoptosis: a review of programmed cell death. Toxicologic pathology *35*, 495–516.

12. Magerl, M., Tobin, D.J., Müller-Röver, S., Hagen, E., Lindner, G., McKay, I.A., and Paus, R. (2001). Patterns of Proliferation and Apoptosis during Murine Hair Follicle Morphogenesis. Journal of Investigative Dermatology *116*, 947–955.

13. Berghe, T. Vanden, Linkermann, A., Jouan-Lanhouet, S., Walczak, H., and Vandenabeele, P. (2014). Regulated necrosis: the expanding network of non-apoptotic cell death pathways. Nature Reviews Molecular Cell Biology *15*, 135–47.

14. Hamer, P.W., McGeachie, J.M., Davies, M.J., and Grounds, M.D. (2002). Evans Blue Dye as an in vivo marker of myofibre damage: optimising parameters for detecting initial myofibre membrane permeability. Journal of Anatomy *200*, 69–79.

15. Matsuda, R., Nishikawa, A., and Tanaka, H. (1995). Visualization of dystrophic muscle fibers in mdx mouse by vital staining with Evans blue: evidence of apoptosis in dystrophin-deficient muscle. Journal of biochemistry *118*, 959–64.

16. Arnold, L., Henry, A., Poron, F., Baba-Amer, Y., van Rooijen, N., Plonquet, A., Gherardi, R.K., and Chazaud, B. (2007). Inflammatory monocytes recruited after skeletal muscle injury switch into antiinflammatory macrophages to support myogenesis. The Journal of experimental medicine *204*, 1057–69.

17. Londhe, P., and Guttridge, D.C. (2015). Inflammation induced loss of skeletal muscle. Bone *80*, 131–42.

18. Tidball, J.G., and Wehling-Henricks, M. (2007). Macrophages promote muscle membrane repair and muscle fibre growth and regeneration during modified muscle loading in mice in vivo. The Journal of physiology *578*, 327–36.

19. Borisov, A.B., Martynova, M.G., and Russell, M.W. (2008). Early incorporation of obscurin into nascent sarcomeres: implication for myofibril assembly during cardiac myogenesis. Histochemistry and cell biology *129*, 463–78.

20. Raeker, M.Ö., Shavit, J.A., Dowling, J.J., Michele, D.E., and Russell, M.W. (2014). Membrane-myofibril cross-talk in myofibrillogenesis and in muscular dystrophy pathogenesis: lessons from the zebrafish. Frontiers in Physiology *5*, 14.

21. Sanger, J.W., Kang, S., Siebrands, C.C., Freeman, N., Du, A., Wang, J., Stout, A.L., and Sanger, J.M. (2006). How to build a myofibril. Journal of Muscle Research and Cell Motility *26*, 343–354.

22. Mann, C.J., Perdiguero, E., Kharraz, Y., Aguilar, S., Pessina, P., Serrano, A.L., and Muñoz-Cánoves, P. (2011). Aberrant repair and fibrosis development in skeletal muscle. Skelet Muscle *1*, 21.

23. Bär, H., Strelkov, S. V, Sjöberg, G., Aebi, U., and Herrmann, H. (2004). The biology of desmin filaments: how do mutations affect their structure, assembly, and organisation? Journal of structural biology *148*, 137–52.

24. Goldfarb, L.G., Olive, M., Vicart, P., and Goebel, H.H. (2008). Intermediate filament diseases: desminopathy. In The sarcomere and skeletal muscle disease, N. G. Laing, ed. (New York, NY: Landes Biosciences and Springer Science+Business Media, LLC), pp. 131–160.

25. Capetanaki, Y., Papathanasiou, S., Diokmetzidou, A., Vatsellas, G., and Tsikitis, M. (2015). Desmin related disease: A matter of cell survival failure. Current Opinion in Cell Biology *32*, 113–120.

26. Volodin, A., Kosti, I., Goldberg, A.L., and Cohen, S. (2017). Myofibril breakdown during atrophy is a delayed response requiring the transcription factor PAX4 and desmin depolymerization. Proceedings of the National Academy of Sciences *114*, E1375–E1384.

27. Schiaffino, S., Dyar, K.A., Ciciliot, S., Blaauw, B., and Sandri, M. (2013). Mechanisms regulating skeletal muscle growth and atrophy. FEBS Journal *280*, 4294–4314.

28. Bodine, S.C., and Baehr, L.M. (2014). Skeletal muscle atrophy and the E3 ubiquitin ligases MuRF1 and MAFbx/atrogin-1. American journal of physiology. Endocrinology and metabolism *307*, E469–84.

29. Huang, A.H., Riordan, T.J., Wang, L., Eyal, S., Zelzer, E., Brigande, J. V, and Schweitzer, R. (2013). Repositioning forelimb superficialis muscles: tendon attachment and muscle activity enable active relocation of functional myofibers. Developmental cell *26*, 544–51.

30. Bonaldo, P., Sandri, M., Allen, D.L., Unterman, T.G., Amirouche, A., Durieux, A.C., Banzet, S., Koulmann, N., Bonnefoy, R., Mouret, C., *et al.* (2013). Cellular and molecular mechanisms of muscle atrophy. Disease models & mechanisms *6*, 25–39.

31. Sakuma, K., Aoi, W., and Yamaguchi, A. (2015). Current understanding of sarcopenia: possible candidates modulating muscle mass. Pflügers Archiv - European Journal of Physiology *467*, 213–229.

32. von Haehling, S., Ebner, N., dos Santos, M.R., Springer, J., and Anker, S.D. (2017). Muscle wasting and cachexia in heart failure: mechanisms and therapies. Nature Reviews Cardiology *14*, 323–341.

33. Moschella, M.C., and Ontell, M. (1987). Transient and chronic neonatal denervation of murine muscle: a procedure to modify the phenotypic expression of muscular dystrophy. Journal of Neuroscience *7*, 2145–2152.

34. Yang, X., Arber, S., William, C., Li, L., Tanabe, Y., Jessell, T.M., Birchmeier, C., and Burden, S.J. (2001). Patterning of muscle acetylcholine receptor gene expression in the absence of motor innervation. Neuron *30*, 399–410.

35. Bruusgaard, J.C., and Gundersen, K. (2008). In vivo time-lapse microscopy reveals no loss of murine myonuclei during weeks of muscle atrophy. The Journal of Clinical Investigation *118*, 1450–1457.

36. Huang, A.H., Riordan, T.J., Pryce, B., Weibel, J.L., Watson, S.S., Long, F., Lefebvre, V., Harfe, B.D., Stadler, H.S., Akiyama, H., *et al.* (2015). Musculoskeletal integration at the wrist underlies the modular development of limb tendons. Development *142*, 2431–2441.

37. Green, D.R. (2005). Apoptotic Pathways: Ten Minutes to Dead. Cell *121*, 671–674.

38. Galluzzi, L., Maiuri, M.C., Vitale, I., Zischka, H., Castedo, M., Zitvogel, L., and Kroemer, G. (2007). Cell death modalities: classification and pathophysiological implications. Cell Death and Differentiation *14*, 1237–1243.

39. Gallant, J.R., Traeger, L.L., Volkening, J.D., Moffett, H., Chen, P.-H., Novina, C.D., Phillips, G.N., Anand, R., Wells, G.B., Pinch, M., *et al.* (2014). Nonhuman genetics. Genomic basis for the convergent evolution of electric organs. Science (New York, N.Y.) *344*, 1522–5.

40. Unguez, G.A., and Zakon, H.H. (1998). Reexpression of myogenic proteins in mature electric organ after removal of neural input. The Journal of neuroscience : the official journal of the Society for Neuroscience *18*, 9924–35.

41. Heredia, J.E., Mukundan, L., Chen, F.M., Mueller, A.A., Deo, R.C., Locksley, R.M., Rando, T.A., and Chawla, A. (2013). Type 2 innate signals stimulate fibro/adipogenic progenitors to facilitate muscle regeneration. Cell *153*, 376–388.

42. Joe, A.W.B., Yi, L., Natarajan, A., Le Grand, F., So, L., Wang, J., Rudnicki, M.A., and Rossi, F.M. V. (2010). Muscle injury activates resident fibro/adipogenic progenitors that facilitate myogenesis. Nature Cell Biology *12*, 153–163.

43. Monks, J., Rosner, D., Jon Geske, F., Lehman, L., Hanson, L., Neville, M.C., and Fadok, V.A. (2005). Epithelial cells as phagocytes: apoptotic epithelial cells are engulfed by mammary alveolar epithelial cells and repress inflammatory mediator release. Cell Death Differ *12*, 107–114.

44. Schwegler, M., Wirsing, A.M., Dollinger, A.J., Abendroth, B., Putz, F., Fietkau, R., and Distel, L.V. (2015). Clearance of primary necrotic cells by non-professional phagocytes. Biol. Cell *107*, 372–387.

45. Souza, M.V., Van Weeren, P.R., Van Schie, H.T.M., and Van De Lest, C.H.A. (2010). Regional differences in biochemical, biomechanical and histomorphological characteristics of the equine suspensory ligament. Equine Veterinary Journal *42*, 611–620.

46. Gibbons, M.C., Singh, A., Anakwenze, O., Cheng, T., Pomerantz, M., Schenk, S., Engler, A.J., and Ward, S.R. (2017). Histological Evidence of Muscle Degeneration in Advanced Human Rotator Cuff Disease. J Bone Joint Surg Am *99*, 190–199.

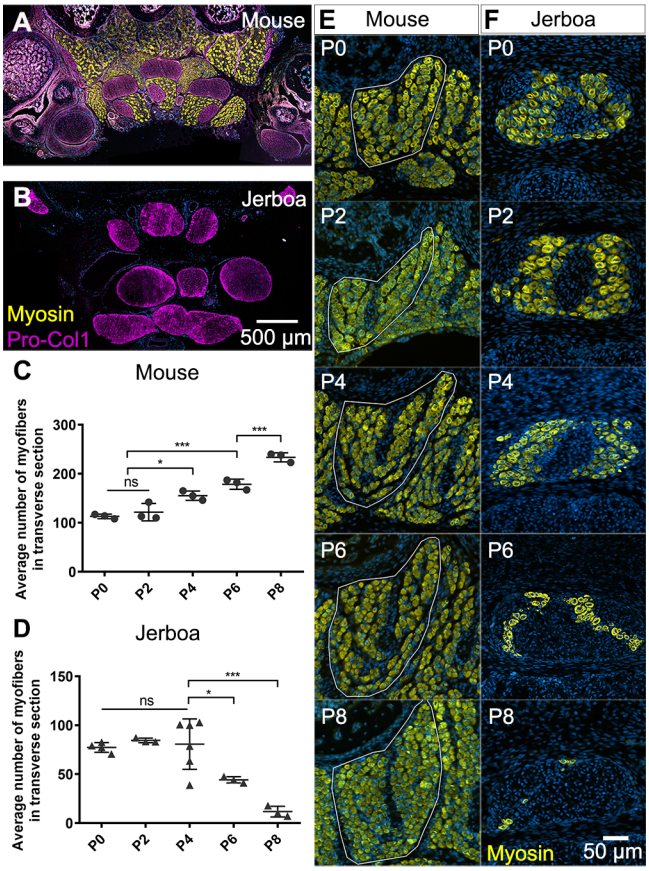

Figure 1: Muscles are rapidly lost in the neonatal jerboa foot.
(A and B) Transverse sections of adult (A) mouse and (B) jerboa foot.
(C and D) Mean and standard deviation of the number of myofibers in transverse sections of third digit interosseous muscle at two-day intervals from birth to postnatal day 8. (C) Mouse P0-P8, n=3 animals each. (D) Jerboa P0, n=4 animals; P2, P6, P8, n=3 animals each; P4, n=6 animals. (*$p<0.05$, **$p<0.01$, ***$p<0.001$).
(E and F) Representative transverse sections of interosseous muscle of the third digit of (E) mouse and (F) jerboa. For all: top dorsal; bottom ventral. See also Figure S1.

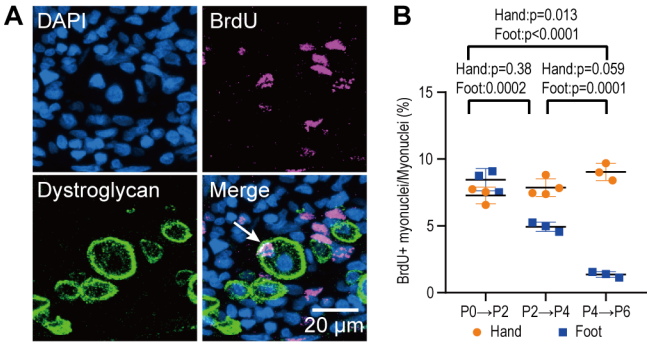

Figure 2: The rate of myocyte fusion is reduced prior to myofiber loss. (A) Newly fused myocyte nuclei within Dystroglycan+ myofiber membranes (arrowheads) can be disitinguished two days after labeling with BrdU. (C) The mean and standard deviation of BrdU+ myonuclei (putative fusion events) normalized to all myofiber nuclei in jerboa hand and foot muscles at intervals from P0 to P6. Foot at P0-P2, P2-P4, P4-P6, Hands at P0-P2, P4-P6, n=3 animals each; Hands at P2-P4, n=4 animals each. See also Figure S1.

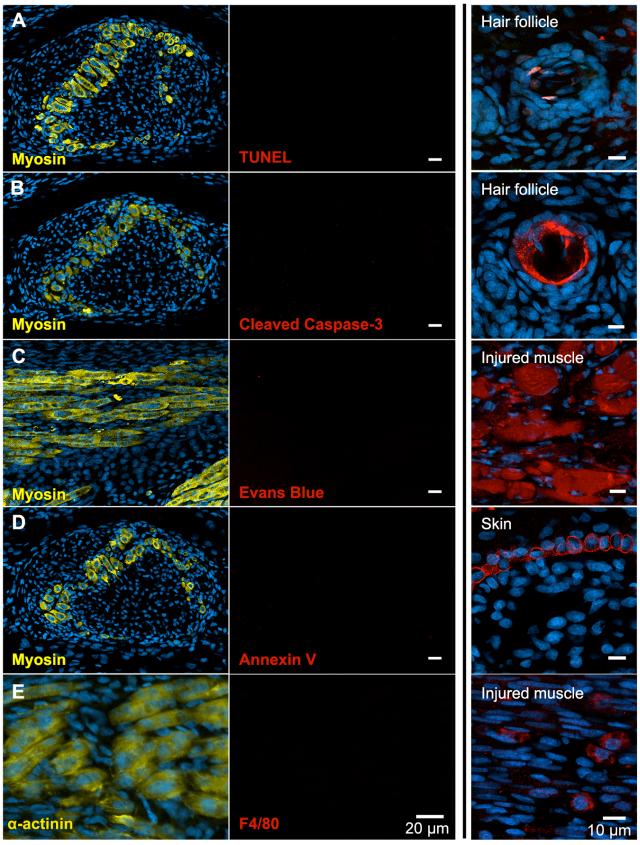

Figure 3: There is no evidence of apoptosis, necrosis, or macrophage infiltration.
(A and B) TUNEL and cleaved Caspase-3 staining for apoptotic nuclei in transverse sections of third digit interosseous muscle in the P6 jerboa foot and of positive control (TUNEL, n=3 animals; cleaved Caspase-3, n=2 animals). See also Figure S2.
(C) EBD detection in longitudinal section of third digit interosseous muscle in the P5 jerboa foot and of positive control (n=5 animals). See also Figure S3.
(D) Annexin V immunofluorescence in longitudinal section of third digit interosseous muscle in the P6 jerboa foot and of positive control (n=3 animals). See also Figure S3.
(E) F4/80 immunofluorescence in longitudinal section of third digit interosseous muscle in the P6 jerboa foot and of positive control (n=2 animals). See also Figure S4.

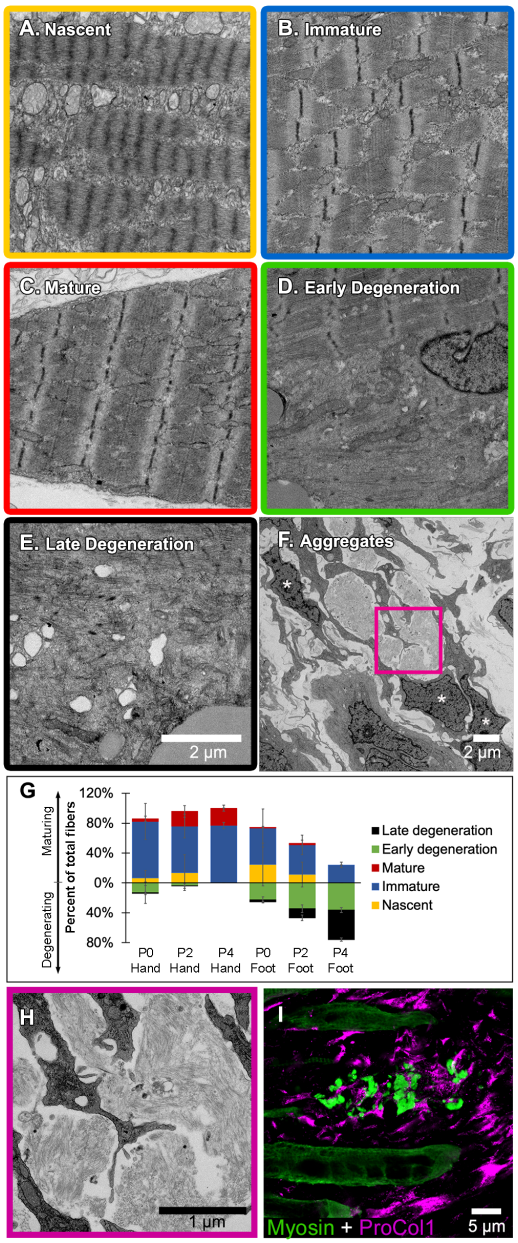

Figure 4: Jerboa foot myofibers degenerate from a nascent state soon after birth.

(A to C) TEM of representative jerboa hand myofibers illustrating categories (A) nascent, (B) immature, and (C) mature.

(D and E) TEM of Representative jerboa foot myofibers illustrating categories (D) early degeneration and (E) late degeneration. Scale bar in E is also for A to D.

(F) TEM of filamentous aggregates and surrounding fibroblast-like cells (asterisks) observed in jerboa feet.

(G) Mean percentage and standard deviation of myofibers in each category in jerboa P0, P2, P4 hand and foot muscles. Number of myofibers pooled from three animals at each stage: hand – (P0), n=135; (P2), n=195; (P4), n=184 (P4); foot – (P0), n=186; (P2), n=193; (P4), n=186.

(H) Higher magnification image of myofibril aggregates in F.

(I) Pro-Collagen I positive cells surround skeletal muscle myosin^{+} aggregates in jerboa feet.

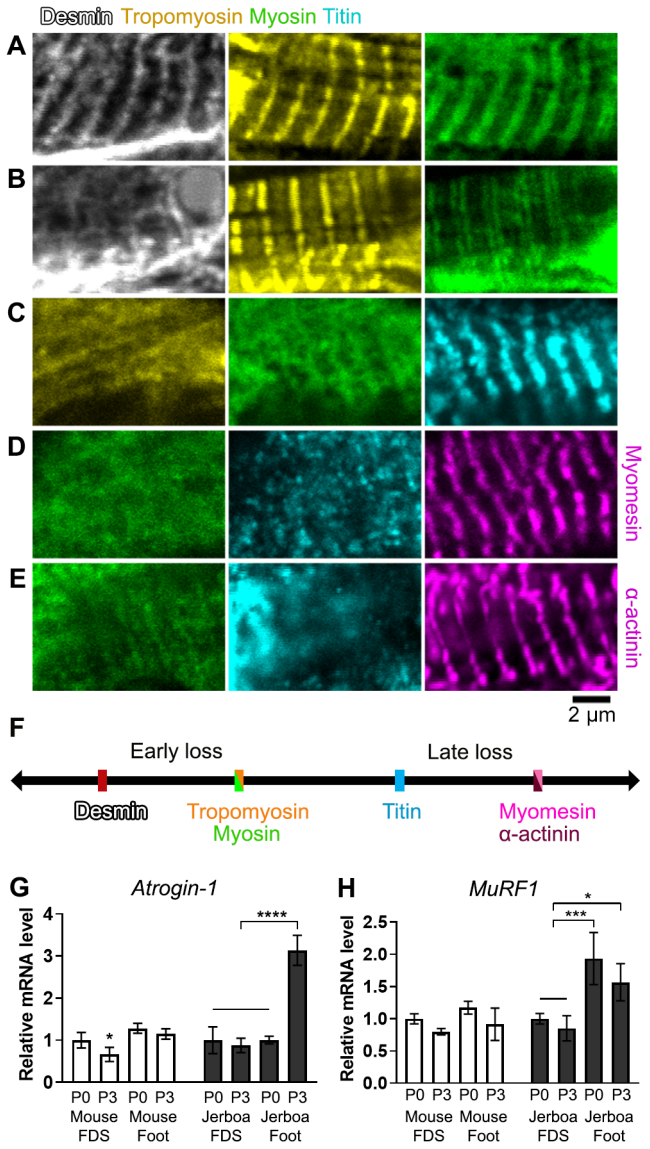

Figure 5: Sarcomere disorganization and E3 ubiquitin ligase expression suggest an "atrophy-like" mechanism of jerboa foot muscle loss.

(A to E) Multicolor immunofluorescence images of sarcomere protein organization in P4 jerboa foot muscles (representative of 704 myofibers from seven P4 animals).

(F) Model of the interpreted order of sarcomere protein disorganization derived from Tables S1-5.

(G and H) RT-qPCR measurements of *Atrogin-1/MAFbx* (G) and *MuRF1* (H) mRNA normalized to *SDHA*. Fold-change and standard deviations are expressed relative to the mean for P0 forearm muscle (FDS) of the same species. (*p<0.05, ***p<0.001, ****p<0.0001). Mouse P0 FDS (n=5), foot (n=4); mouse P3 FDS (n=3), foot (n4); jerboa P0 FDS (n=6), foot (n=5); jerboa P3 FDS (n=4), foot (n=6). See also Figure S5.